COMPDYN 2011
ECCOMAS Thematic Conference on
Computational Methods in Structural Dynamics and Earthquake Engineering
M. Papadrakakis, M. Fragiadakis, V. Plevris (eds.)
Corfu, Greece, 25-28 May 2011

VERIFICATION OF AN EMPIRICAL PREDICTION METHOD FOR GROUND BORNE VIBRATIONS IN BUILDINGS DUE TO HIGH SPEED RAILWAY TRAFFIC

H. Verbraken[1], **S. François**[1], **G. Degrande**[1], **G. Lombaert**[1]

[1]Department of Civil Engineering, K.U.Leuven
Kasteelpark Arenberg 40, B-3001 Leuven, Belgium
e-mail: {hans.verbraken,stijn.francois,geert.degrande,geert.lombaert}@bwk.kuleuven.be

Keywords: Railway induced vibration, Empirical predictions; Dynamic soil–structure interaction

Abstract. *Ground borne vibration in buildings due to railway traffic is a major concern in densely built up areas. In practice, railway induced vibration is often predicted by means of empirical methods such as the Detailed Vibration Assessment developed by the U.S. Federal Railroad Administration (FRA). The vibration velocity level in a building is predicted based on a separate characterization of the source, the wave propagation and the receiver. They are characterized by a force density, a line transfer mobility and a coupling loss factor, respectively. While the line transfer mobility is determined directly with in situ measurements of transfer functions, the force density and the coupling loss factor are obtained indirectly. In this paper, a numerical model is used to simulate the experimental FRA procedure. The influence of the soil properties on the coupling loss factor is investigated by computing the coupling loss factor on three sites with different soil conditions. Each coupling loss factor is used to predict the vibration velocity level and the result is compared to a numerical prediction such that the accuracy of the procedure can be investigated. It turns out that the soil has a large influence on the coupling loss factor, as the reduction of the vibration velocity level between the free field and the foundation is affected by the relative stiffness of the building and the soil. Furthermore, the coupling loss factor strongly depends on the position of the point where it has been measured.*

1 Introduction

Ground borne vibration in buildings due to railway traffic is a major concern in densely built up areas. At low frequencies (1–80 Hz), vibration in buildings is perceived by the occupants as mechanical vibration, whereas at higher frequencies (16–250 Hz), it is perceived as re-radiated noise. An accurate prediction of this vibration is required so that effective mitigation measures can be taken.

The numerical modeling of vibration in building is a problem of dynamic soil–structure interaction. Generally, the coupling between the source and the receiver can be neglected such that a prediction in two steps is possible. First, the dynamic load is determined at the source and the vibration in the free field is computed. Second, the free field vibration is imposed as the incident wave field and the building response is computed. Several numerical models have been developed for the prediction of free field vibration due to railway traffic at grade [1, 2] at the source side and the building response at the receiver side. The validation of these models show that a good knowledge of all relevant input parameters is necessary to obtain reliable predictions. In practice, empirical predictions where these parameters are inherently taken into account are therefore often used. The Federal Railroad Administration (FRA) and the Federal Transit Administration (FTA) of the U.S. Department of Transportation have developed a set of empirical procedure to predict vibration levels due to railway traffic [3, 4]. Three different levels of assessment are described: the Screening procedure, the Generalized Vibration Assessment and the Detailed Vibration Assessment. The first two levels are used for general screening purposes. The third level is based on a prediction technique developed by Bovey [5] and Nelson and Saurenman [6] and presents a more elaborate method based on field measurements.

The Detailed Vibration Assessment predicts the vibration velocity level $\mathrm{L_v}$ $[\mathrm{dB\,ref\,}10^{-8}\,\mathrm{m/s}]$ (root mean square in one-third octave bands) with the following equation:

$$\mathrm{L_v} = \mathrm{L_F} + \mathrm{TM_L} + \mathrm{C_{build}} \tag{1}$$

The first term in equation (1) is the force density $\mathrm{L_F}$ $[\mathrm{dB\,ref\,1\,N}/\sqrt{\mathrm{m}}]$ and is a measure for the power per unit length radiated by the source. The second term is the line transfer mobility $\mathrm{TM_L}$ $[\mathrm{dB\,ref\,}10^{-8}\,\frac{\mathrm{m/s}}{\mathrm{N}/\sqrt{\mathrm{m}}}]$ and is a measure for the vibration energy that is transmitted through the soil relative to the power per unit length radiated by the source. The third term is the coupling loss factor $\mathrm{C_{build}}$ $[\mathrm{dB}]$ and is a measure for the modification of vibration spectrum due to the dynamic interaction between the foundation and the soil. Each term in equation (1) is determined experimentally.

The line transfer mobility $\mathrm{TM_L}$ is determined with an experimental measurement of transfer functions between the track and the free field (Figure 1). The point transfer mobility $\mathrm{TM_{P}}_k$ $[\mathrm{dB\,ref\,}10^{-8}\,\frac{\mathrm{m/s}}{\mathrm{N}}]$ is measured as the transfer function between the applied force in a single impact point k and the velocity in the free field. The line transfer mobility $\mathrm{TM_L}$ is obtained as the superposition of different point transfer mobilities, determined along the track alignment:

$$\mathrm{TM_L} = 10\log_{10}\left(L_\mathrm{a}\sum_{k=1}^{n} 10^{\frac{\mathrm{TM_P}_k}{10}}\right) \tag{2}$$

where L_a is the distance between the impact points and n is the total number of impact points.

The force density $\mathrm{L_F}$ is determined indirectly based on equation (1). The vibration velocity level during a train passage is measured in the free field (without the presence of a building). The line transfer mobility $\mathrm{TM_L}$ is determined experimentally and is subtracted from the free

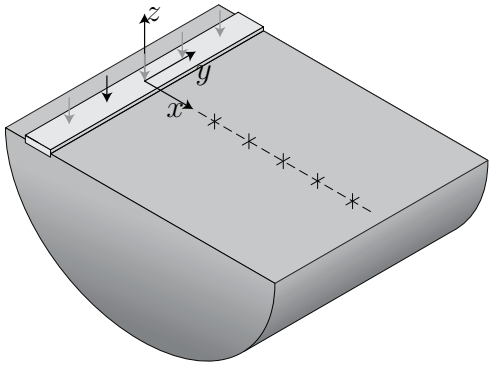

Figure 1: The experimental setup for the determination of the line transfer mobility $\mathrm{TM_L}$.

field vibration velocity level, resulting in a normalized force density $\mathrm{L_F}$ of the train passage. The force density is not only determined, however, by the dynamic characteristics of the train and the track, but also depends on the subsoil conditions.

The coupling loss factor $\mathrm{C_{build}}$ is determined indirectly as the relation between the vibration velocity level in the free field and the vibration velocity level at the foundation of a building. The coupling loss factor depends on the building and foundation type, but also on the subsoil conditions. In the FRA manual, a frequency dependent coupling loss factor is proposed for several building and foundation types.

In a prediction with the FRA procedure, each term in equation (1) is determined experimentally. When a new building is constructed in the neighborhood of an existing track, the vibration velocity level in the building is predicted as follows. The force density $\mathrm{L_F}$ and the line transfer mobility $\mathrm{TM_L}$ are measured on site. The advantage is that the source and the local transfer of vibration are correctly accounted for. The coupling loss factor $\mathrm{C_{build}}$ cannot be determined on site, however, as no building is present yet. It can be obtained from a database that contains previous measurements of the coupling loss factor of several building types. Examples of coupling loss factors are also given in de FRA manual [3]. The coupling loss factor is not only determined by the building or foundation type but also by the subsoil conditions, however. It is therefore important that the conditions of the soil are similar at the site where the coupling loss factor has been determined and at the site where it will be applied.

When a prediction is needed on a site with an existing building and a new track, the line transfer mobility $\mathrm{TM_L}$ and the coupling loss factor $\mathrm{C_{build}}$ are determined on site, whereas the force density $\mathrm{L_F}$ has to be determined at another site with similar conditions for the train, the track and the soil.

In the present paper, the influence of the soil characteristics on the coupling loss factor is investigated by numerical simulations to assess possible inaccuracies in the prediction due to a mismatch in the soil conditions. The influence of the soil conditions on the force density has been investigated previously [7]. In section 2, the numerical model is introduced. The vibration velocity level in the free field and in the building is computed numerically on three different soils in section 4 and section 5. In section 6, the coupling loss factor at each soil type is obtained from these results. Finally, in section 7, a prediction of the vibration velocity level in the building is made by combining the computed coupling loss factors for each soil type with the free field vibration velocity level at another site. The predictions are compared to the exact solution and the accuracy of the FRA procedure is evaluated.

2 Numerical model

A numerical model is used to compute the vibration velocity in a building due to a train passage on a railway track. The source and receiver are considered to be weakly coupled such that a prediction in two steps is possible. First, the vibration velocity in the free field due to moving loads is computed. Therefore, the axle loads of the moving train and the transfer functions from the track to the free field need to be determined. Second, the response of the building is computed based on the incident wavefield.

2.1 Source model

Figure 2 shows the coupled track–soil domain Ω of the source system, which is subdivided into the soil subdomain Ω_s and the track subdomain Ω_b, connected at the interface Σ_bs. Tractions $\bar{\mathbf{t}}_\mathrm{b}$ are imposed at the boundary $\Gamma_{\mathrm{b}\sigma}$. In case of a train passage, these tractions represent the axle loads.

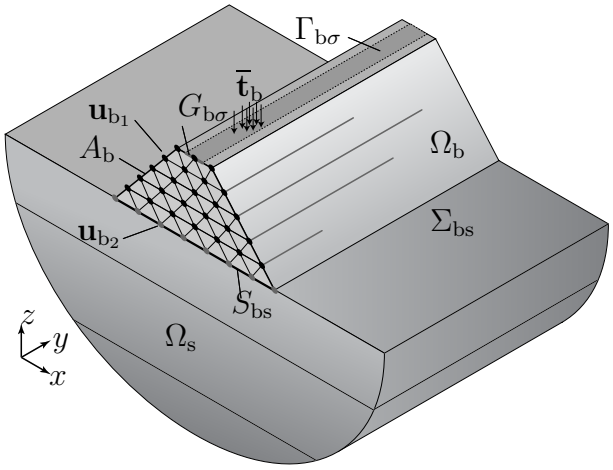

Figure 2: The geometry of the coupled track–soil system.

The vibration velocity $\mathbf{v}(\mathbf{x}', t)$ at a point $\mathbf{x}'$ in the free field due to k moving axle loads $\mathbf{g}_k(t)$ is calculated with the following convolution integral [1, 8]:

$$\mathbf{v}(\mathbf{x}', t) = \sum_{k=1}^{n_\mathrm{a}} \int_{-\infty}^{t} \mathbf{H}^\mathrm{T}(\mathbf{x}_k(\tau), \mathbf{x}', t-\tau)\mathbf{g}_k(\tau)d\tau \tag{3}$$

Each element $h_{ij}(\mathbf{x}', \mathbf{x}, t)$ of the matrix $\mathbf{H}(\mathbf{x}', \mathbf{x}, t)$ represents the velocity at a point $\mathbf{x}$ in the direction $\mathbf{e}_j$ at time t due to an impulsive load at a point $\mathbf{x}'$ in the direction $\mathbf{e}_i$ at time $t = 0$. In equation (3), dynamic reciprocity is used to replace the matrix $\mathbf{H}(\mathbf{x}', \mathbf{x}, t)$ by $\mathbf{H}^\mathrm{T}(\mathbf{x}, \mathbf{x}', t)$.

In the following, a longitudinal invariant track and a horizontally layered soil are assumed such that the geometry of the domain Ω is invariant in the longitudinal direction $\mathbf{e}_y$. In this case, the transfer function is unaffected by an arbitrary translation $l\mathbf{e}_y$ of the source and the receiver position. If l equals $y_{k0} + v\tau$, the source position $\mathbf{x}_k(\tau) - l\mathbf{e}_y = \{x_{k0}, 0, z_{k0}\}^\mathrm{T}$ no longer depends on the time τ and can be omitted in the argument of the transfer function. Furthermore, the coordinates x' and z' of the receiver position $\mathbf{x}' = \{x', y', z'\}^\mathrm{T}$ are assumed to

be fixed, so that equation (3) is rewritten as follows:

$$\mathbf{v}(y',t) = \sum_{k=1}^{n_\mathrm{a}} \int_{-\infty}^{t} \mathbf{H}^\mathrm{T}(y' - y_{k0} - v\tau, t-\tau)\mathbf{g}_k(\tau)d\tau \tag{4}$$

Because the domain is longitudinally invartiant, a double forward Fourier transform from the space–time domain (y',t) allows for an expression of the vibration velocity in the wavenumber–frequency domain (k_y,ω):

$$\tilde{\mathbf{v}}(k_y,\omega) = \sum_{k=1}^{n_\mathrm{a}} \tilde{\mathbf{H}}^\mathrm{T}(k_y,\omega)\hat{\mathbf{g}}_k(\omega - k_y v)\exp(+ik_y y_{k0}) \tag{5}$$

where a hat denotes the representation in the space–frequency domain and a tilde the representation in the wavenumber–frequency domain. An inverse wavenumber transform results in the frequency content $\hat{\mathbf{v}}(y',\omega)$ of the vibration velocity.

The transfer matrix $\tilde{\mathbf{H}}^\mathrm{T}(k_y,\omega)$ in equation (5) is formulated in the wavenumber–frequency domain. It is computed with a 2.5D coupled finite element – boundary element method [9], where the longitudinal invariance of the domain is exploited by a Fourier transform from the direction y' to the wavenumber k_y. A finite element model for the track is coupled to a boundary element model for the soil.

The dynamic axle loads $\hat{\mathbf{g}}_k(\omega)$ in equation (5) are the result of the interaction between the vehicle, the track and the soil. They are computed in the frequency domain by means of a compliance formulation in a moving frame of reference [8], based on a perfect contact between the wheels and the track.

2.2 Receiver model

Figure 3 shows the coupled soil–structure domain Ω of the receiver system, which is subdivided into the soil subdomain Ω_s and the structure subdomain Ω_b, connected at the interface Σ_bs.

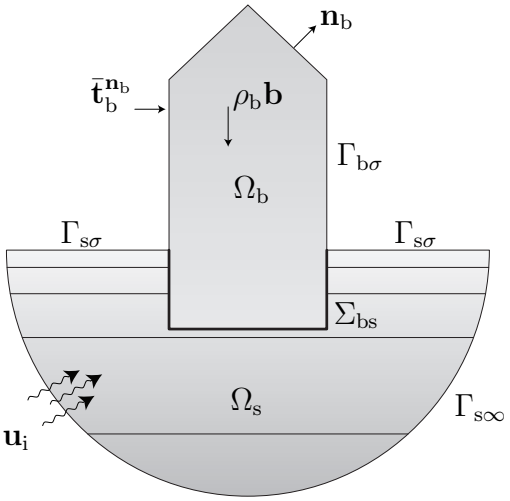

Figure 3: The geometry of the coupled soil–structure system.

The calculation of the vibration velocity in the building due to an incident wavefield is a problem of dynamic soil–structure interaction. The problem is assumed to be linear and all equation are elaborated in the frequency domain.

For any virtual displacement field $\hat{\mathbf{v}}_\mathrm{b}$ imposed on the structure Ω_b, the sum of the virtual work of the internal and the inertial forces is equal to the virtual work of the external loads:

$$-\omega^2 \int_{\Omega_\mathrm{b}} \hat{\mathbf{v}}_\mathrm{b} \cdot \rho_\mathrm{b} \hat{\mathbf{u}}_\mathrm{b} d\Omega + \int_{\Omega_\mathrm{b}} \hat{\boldsymbol{\epsilon}}_\mathrm{b}(\hat{\mathbf{v}}_\mathrm{b}) : \hat{\sigma}_\mathrm{b}(\hat{\mathbf{u}}_\mathrm{b}) d\Omega = \int_{\Omega_\mathrm{b}} \hat{\mathbf{v}}_\mathrm{b} \cdot \rho_\mathrm{b} \hat{\mathbf{b}} d\Omega + \int_{\Gamma_{\mathrm{b}\sigma}} \hat{\mathbf{v}}_\mathrm{b} \cdot \hat{\bar{\mathbf{t}}}_\mathrm{b}^{\mathbf{n}_\mathrm{b}} d\Gamma + \int_{\Sigma_\mathrm{bs}} \hat{\mathbf{v}}_\mathrm{b} \cdot \hat{\mathbf{t}}_\mathrm{b}^{\mathbf{n}_\mathrm{b}}(\hat{\mathbf{u}}_\mathrm{b}) d\Gamma \quad (6)$$

where $\hat{\mathbf{u}}_\mathrm{b}$ is the displacement vector in the structure, $\rho_\mathrm{b}\hat{\mathbf{b}}$ denotes the body force in the domain Ω_b, and $\hat{\mathbf{t}}_\mathrm{b}^{\mathbf{n}_\mathrm{b}} = \hat{\sigma}_\mathrm{b} \cdot \mathbf{n}_\mathrm{b}$ is the traction vector on a boundary with unit outward normal vector $\mathbf{n}_\mathrm{b}$. Tractions $\hat{\bar{\mathbf{t}}}_\mathrm{b}^{\mathbf{n}_\mathrm{b}}$ are imposed on the boundary $\Gamma_{\mathrm{b}\sigma}$.

When equation (6) is discretized by means of 3D finite elements and the equilibrium of stresses on the interface Σ_bs is accounted for, the following expression is obtained [9]:

$$\left(\mathbf{K}_\mathrm{bb} - \omega^2 \mathbf{M}_\mathrm{bb} + \hat{\mathbf{K}}_\mathrm{bb}^\mathrm{s}(\omega)\right) \hat{\mathbf{u}}_\mathrm{b} = \hat{\mathbf{f}}_\mathrm{b}(\omega) + \hat{\mathbf{f}}_\mathrm{b}^\mathrm{s}(\omega) \quad (7)$$

where $\mathbf{K}_\mathrm{bb}$ and $\mathbf{M}_\mathrm{bb}$ are the finite element stiffness and mass matrix, $\hat{\mathbf{K}}_\mathrm{bb}^\mathrm{s}(\omega)$ is the dynamic soil stiffness matrix, $\hat{\mathbf{f}}_\mathrm{b}(\omega)$ is the external load vector and $\hat{\mathbf{f}}_\mathrm{b}^\mathrm{s}(\omega)$ is the force vector due to the incident wavefield. The dynamic soil stiffness matrix $\hat{\mathbf{K}}_\mathrm{bb}^\mathrm{s}(\omega)$ and the force vector $\hat{\mathbf{f}}_\mathrm{b}^\mathrm{s}(\omega)$ account for the interaction with the soil and for the incident wavefield, respectively, and are computed by means of the boundary element method.

3 Case

In the following sections, the vibration velocity level in the free field and in a building due to a train passage is computed by means of the numerical models introduced in section 2. The coupling loss factor can be determined numerically from these results. By considering different soil types, the influence of a mismatch in the soil conditions on the coupling loss factor and the resulting prediction is investigated. In this section, the characteristics of the train, track, soil and building are discussed.

In the present case, a classical ballasted track [1] is considered with UIC 60 rails supported every 0.60 m by rubber pads on monoblock concrete sleepers. The rails are continuously welded and are fixed with a Pandrol E2039 rail fastening system and supported by resilient studded rubber rail pads (type 5197) with a thickness of 11 mm. Each rail pad is preloaded with a clip toe load of about 20 kN per rail seat. The prestressed concrete monoblock sleepers have a length $l_\mathrm{sl} = 2.50\,\mathrm{m}$, a width $b_\mathrm{sl} = 0.235\,\mathrm{m}$, a height $h_\mathrm{sl} = 0.205\,\mathrm{m}$ and a mass $m_\mathrm{sl} = 300\,\mathrm{kg}$. The track is supported by a porphyry ballast layer (calibre $25/50$, thickness $d = 0.35\,\mathrm{m}$) and a limestone sub-ballast layer (thickness $d = 0.60\,\mathrm{m}$). The density of these ballast layers is $1700\,\mathrm{kg/m^3}$.

The track is modeled as a longitudinally invariant track [1] by means of the 2.5D finite element method, where the dynamics of the rail pads and the mass of the sleepers are uniformly distributed along the track. It has been shown that continuously and discretely supported tracks have similar dynamic behaviour up to about 500 Hz [10]. The rails are modeled as Euler–Bernoulli beams and the rail pads are modeled as continuous spring–damper connections. The sleepers are assumed to be rigid in the plane of the cross section and are modeled as a uniformly distributed mass along the track. The ballast bed is modeled as a set of distributed, independent linear springs and dampers. Figure 4 shows the cross section of the ballasted track model.

The track is supported by a homogeneous halfspace. In order to investigate the influence of the soil properties on the prediction of the vibration velocity level, three sites are considered

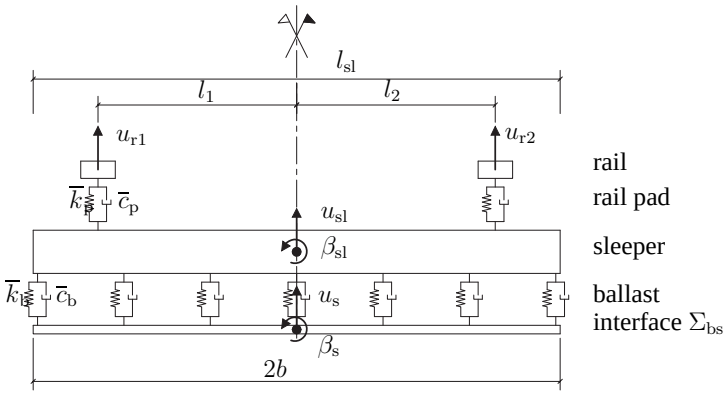

Figure 4: Cross section of a ballasted track model.

with different soil characteristics representing a soft, medium and stiff soil. The dynamic soil characteristics are summarized in Table 1.

Table 1: Dynamic soil characteristics.

Type	C_{s} [m/s]	C_{p} [m/s]	ν [-]	ρ [kg/m^3]	β [-]
Soft	100	200	0.33	1800	0.025
Medium	150	300	0.33	1800	0.025
Stiff	300	600	0.33	1800	0.025

The Thalys HST consists of two locomotives and eight carriages and has a total of 26 axles [8]. Each axle has an unsprung mass $M_{\mathrm{u}} = 2027\,\mathrm{kg}$. The length l of the train equals 200.18 m. The train is modeled as a series of individual axles, as the coupling between different axles through the vehicle can be neglected. The mechanical model of the train therefore only takes into account the unsprung mass M_{u} of each axle.

At 30 m from the track, a masonry building with dimensions $12\,\mathrm{m} \times 6\,\mathrm{m} \times 6\,\mathrm{m}$ is assumed to be present (figure 5a) [11]. The structure has two stories, each subdivided into 4 rooms. The interior and exterior walls have a thickness $t_{\mathrm{w}} = 0.10\,\mathrm{m}$, and consist of clay brick masonry. The floors are concrete slabs with a thickness $t_{\mathrm{fl}} = 0.20\,\mathrm{m}$. All floors are simply supported, corresponding to hinged joints at the slab edges. The structure is founded on a concrete strip foundation with a width $w_{\mathrm{fou}} = 0.60\,\mathrm{m}$ and a thickness $t_{\mathrm{fou}} = 0.20\,\mathrm{m}$. Figure 5b shows the foundation of the building and indicates the location of points A, B, C and D where the response in the free field and in the building will be computed.

The building is modeled with the finite element method. The strip foundation, the walls and the floors are modeled by means of shell elements, using isotropic properties for the foundation and the floors and orthotropic properties for the masonry walls [11]. The lintels above the door and the windows are modeled by means of beam elements.

4 Vibration velocity level in the free field

In this section, the free field response due to the passage of the Thalys HST on the track at a speed of 150 km/h is computed with the source model described in section 2.1. Figure 6 shows the computed time history and the frequency content of the free field vibration velocity in point A due to the passage of the Thalys HST at a speed $v = 150\,\mathrm{km/h}$ on a site with medium soil.

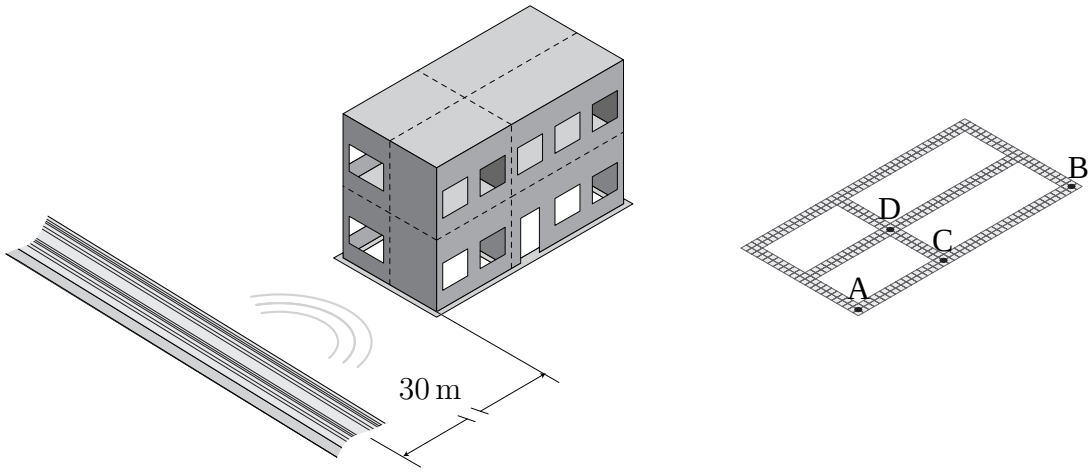

(a) (b)

Figure 5: (a) Geometry and location of the building and (b) foundation of the building and location of the measurement points.

The duration of the passage is about 4.8 s which is approximately equal to the length l of the train divided by the train speed v. The time history can be divided in three parts: an increasing vibration level when the train approaches, a nearly stationary part when the train passes and a decreasing vibration level when the train moves away. The stationary part of the response is selected by means of the DIN selection procedure [12] based on the time T_2 and is indicated in black in Figure 6a. The vibration velocity level $\mathrm{L_v}$ is then defined as the one-third octave band RMS spectrum of the stationary part of the vibration velocity.

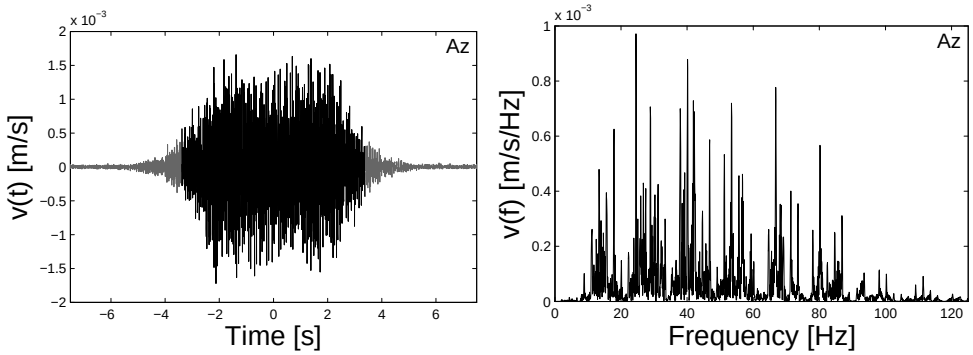

(a) (b)

Figure 6: (a) Time history and (b) frequency content of the vertical velocity at 30 m from the track in the free field due to the passage of a Thalys HST at a speed of 150 km/h on a site with medium soil (stationary part of the time history is indicated in black).

Figure 7 shows the vibration velocity level $\mathrm{L_v}$ at the three different sites in the free field in the points corresponding to point A and point B (Figure 5b). In the response on the stiff soil, a peak around 63 Hz is found. This is due to the resonance of unsprung mass of the wheelsets on the track. In the low frequency range, the highest response is obtained for the soft soil. The response is increasingly attenuated, however, not only at larger distances from the track but also with increasing frequency. As this attenuation is stronger for softer soils, the peak at 63 Hz is

no longer observed in the response on the soft and the medium soil and the highest response in the high frequency range is obtained for the stiff soil.

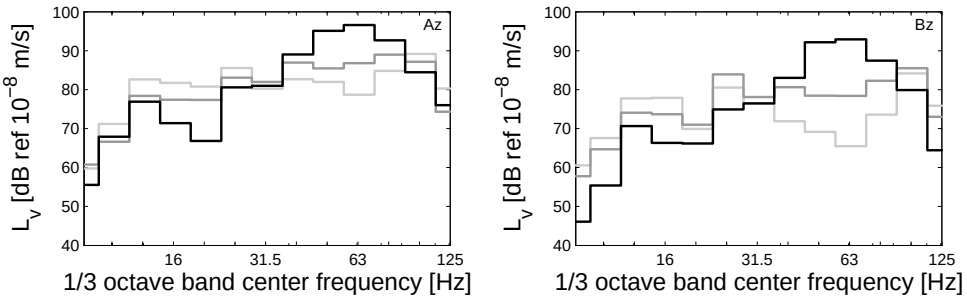

(a) (b)

Figure 7: Free field vibration velocity level at (a) 30 m and (b) 42 m on a soft (light grey line), medium (dark grey line) and stiff (black line) soil.

5 Vibration velocity level in a building

In this section, the response of the building to the passage of the Thalys train on the track is computed with the receiver model described in section 2.2. In Figure 8, the vibration velocity levels at the foundation of the building determined on three different soils are compared. The response is shown at the front side (point A) and at the back side (point B) of the building (Figure 5b), corresponding to the points where the free field response is shown in Figure 7. At low frequencies the highest response is obtained for the soft and the medium soil, whereas at higher frequencies the highest response is obtained for the stiff soil, corresponding to the observation of the vibration velocity level in the same points in the free field. It can be observed, however, that the response at the foundation differs from the response in the free field due to the dynamic soil–structure interaction. This modification is described by the coupling loss factor, discussed in the next section.

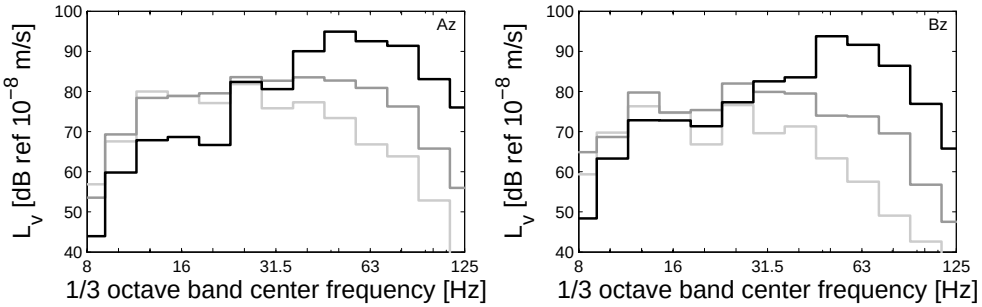

(a) (b)

Figure 8: Vibration velocity level of the foundation in (a) point A and (b) point B on a soft (light grey line), medium (dark grey line) and stiff (black line) soil.

6 Coupling loss factor

The coupling loss factor $\mathrm{C_{build}}$ is determined by subtracting the vibration velocity level $\mathrm{L_F + TM_L}$ in the free field from the vibration velocity level $\mathrm{L_v}$ at the foundation of the building:

$$\mathrm{C_{build} = L_v - (L_F + TM_L)} \tag{8}$$

Figure 9 shows the coupling loss factors in point A and point B, determined at the three different soil types. These values are compared to coupling loss factor proposed in the FRA manual for a 2 to 4 story masonry building. A negative value of the coupling loss factor $\mathrm{C_{build}}$ implies a reduction of the vibration velocity level from the free field to the foundation, while a positive value means an increase of the vibration velocity level.

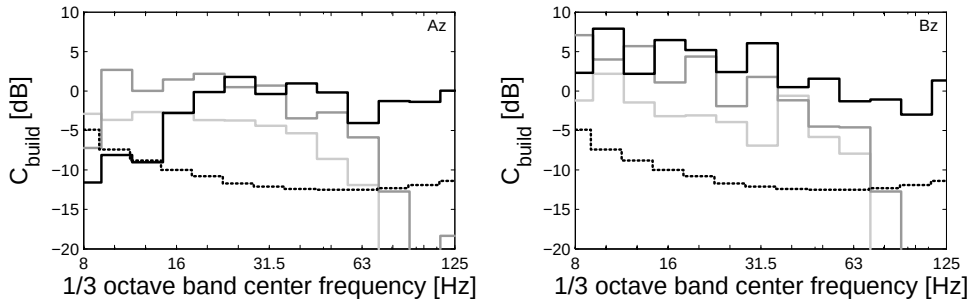

Figure 9: Coupling loss factor $\mathrm{C_{build}}$ in (a) point A and (b) point B on a soft (light grey line), medium (dark grey line) and stiff (black line) soil compared to the curve proposed in the FRA manual for a 2 to 4 story masonry building (dotted line).

In the high frequency range, a zero value is observed for the coupling loss factor for the stiff soil. Due to the high relative stiffness of the soil, the ground vibration is imposed to the building and is transmitted almost unaffectedly to the foundation. A large reduction is observed, however, for the coupling loss factor in the case of the soft and the medium soil. Due to the lower relative stiffness, the ground vibration is transmitted at a reduced level to the foundation. The interaction between the soil and the structure is determined by the characteristic wavelength of the vibration. As the wavelength decreases with increasing frequency and for softer soils, a higher reduction is obtained at high frequencies for the soft and the medium soil.

In the low frequency range, a difference up to 15 dB is observed between the coupling loss factor at the front side (point A) and the back side (point B) of the building. This can be due to the fact that the building response at low frequencies is an average response to the incident wavefield. As the incident wavefield itself is attenuated with increasing distance from the track, a reduction is found at the front side wereas an increase is found at the back side. This effect is more pronounced for the case of the stiff soil.

From the previous discussion it can be concluded that the soil conditions significantly affect the values obtained for the coupling loss factor. Furthermore, it is observed that the computed values for the coupling loss factor overestimate the values proposed by the FRA. The coupling loss factor is also strongly dependent, however, on the location of the measurement point. Figure 10 shows the coupling loss factor determined on the three soils in point C along the edge of the building and in point D in the centre of the building (Figure 5b). The reduction in point D is generally around 10 dB higher than the reduction in point C. The foundation response in a point is affected by the kinematics of the complete building as well as by the local geometry. When torsional and rotational modes of the building are excited, the response at the centre of the foundation is lower. As the incident wavefield is similar in point C and point D, the reduction is higher in point D.

Figure 11a shows the spatial variation over the foundation of the coupling loss factor at 63 Hz, confirming that a higher reduction is obtained in the centre of the building. Furthermore, it is observed that the reduction is generally higher at the front of the building (left side) than

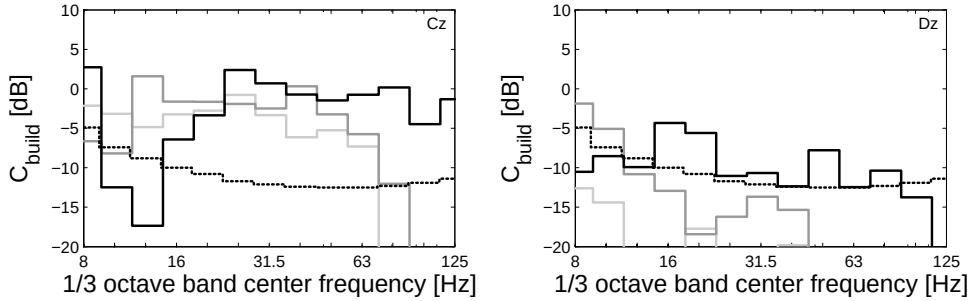

Figure 10: Coupling loss factor C_{build} in (a) point C and (b) point D on a soft (light grey line), medium (dark grey line) and stiff (black line) soil compared to the curve proposed in the FRA manual for a 2 to 4 story masonry building (dotted line).

at the back (right side). Figure 11b shows the average value of the coupling loss factor over all points in the foundation and the 90 % interval of the coupling loss factor values over the foundation. The coupling loss factor is strongly dependent on the location of the measurement point, as a large spread, up to 20 dB, can be observed. The conclusion still holds in case of the average coupling loss factor, however, that the reduction is stronger for softer soils, particularly at higher frequencies.

7 Prediction of the vibration velocity

In this section, a prediction is made for the vibration velocity level at the foundation of a building on a medium soil. In order to investigate the influence of the soil properties on the prediction accuracy, the free field vibration velocity level on a medium soil is therefore combined with the coupling loss factors obtained in section 6. As the coupling loss factor is affected by the position of the measurement point, the average value over the foundation is used. Figure 12 shows the prediction of the response in point A and point B (Figure 5b), compared to a 12 dB region around the exact solution for the medium soil. In case of a coupling loss factor determined on a medium soil, the prediction is generally within 6 dB of the exact solution. In case of a coupling loss factor determined on a soft or a stiff soil, however, the accuracy is significantly less good at higher frequencies. An overestimation of the response up to approximately 20 dB is obtained with the coupling loss factor of the stiff soil, whereas an underestimation up to approximately 15 dB is obtained with the coupling loss factor of the soft soil.

The prediction of the response in point A and B is relatively accurate with an average coupling loss factor determined on the same soil type. Due to the spatial variability, however, it can be expected that the accuracy of the prediction will be less good in other points of the building. Figure 13 shows the prediction of the response for point C and point D (Figure 5b) compared to a 12 dB region around the exact solution. The prediction of the response in point C, located at the edge of the foundation, is relatively accurate when the coupling loss factor of the medium soil is used. The prediction in point D, located in the centre of the foundation, however, is overestimating the response, even when the medium soil coupling loss factor is used.

From the previous analysis, it can be concluded that the coupling loss factor should be determined from data obtained at sites where the conditions for the building, the foundation and the subsoil are similar in order to obtain an accurate prediction. Furthermore, it can be concluded that the location of the measurement point strongly affects the coupling loss factor and

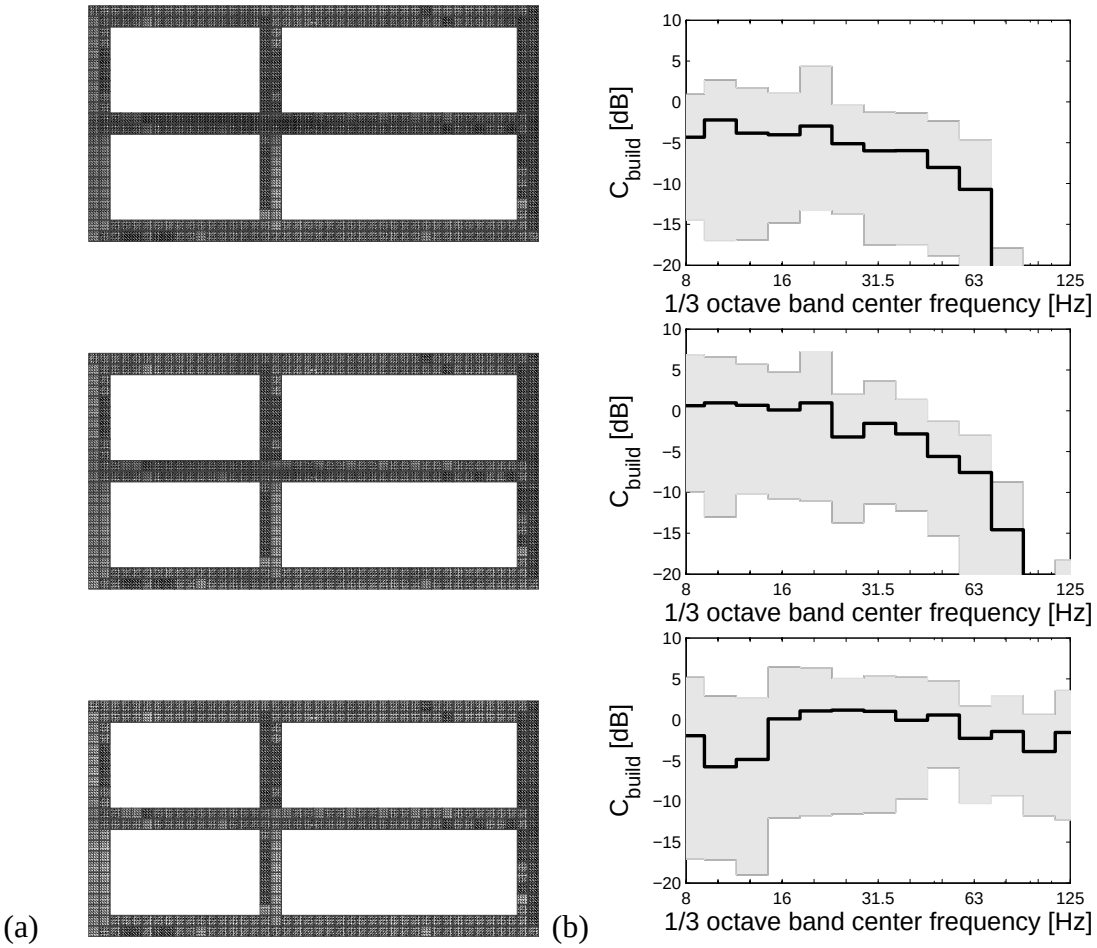

Figure 11: (a) Spatial variation at 63 Hz and (b) average value (black line) and 90 % interval (grey region) of the coupling loss factor $\mathrm{C_{build}}$ on a soft (top), medium (middle) and stiff (bottom) soil.

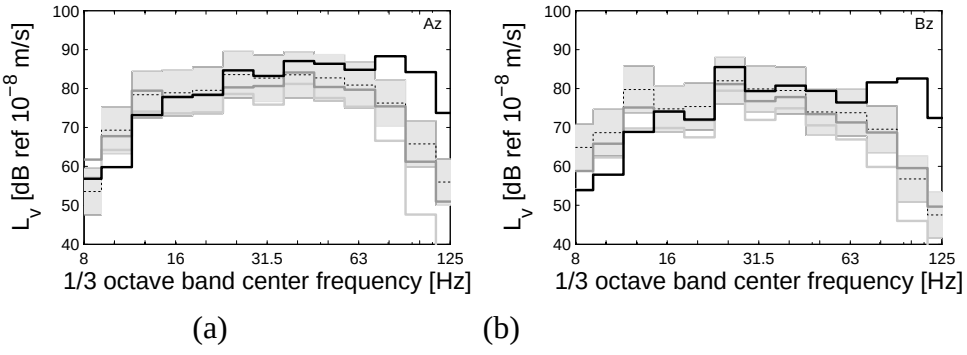

Figure 12: Predicted vibration velocity level in (a) point A and (b) point B using the average coupling loss factor determined on a soft (light grey line), medium (dark grey line) and stiff (black line) soil compared to a 12 dB region (grey region) around the exact solution (dotted black line).

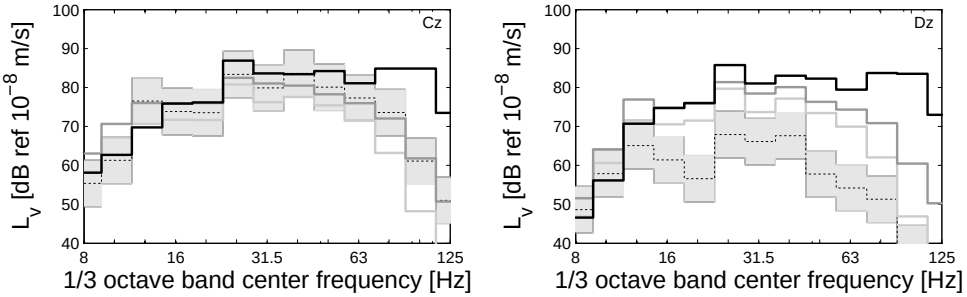

(a) (b)

Figure 13: Predicted vibration velocity level in (a) point C and (b) point D using the average coupling loss factor determined on a soft (light grey line), medium (dark grey line) and stiff (black line) soil.

the resulting prediction of the vibration velocity level. In a prediction with the FRA procedure, an experimental value obtained from previous measurements of the coupling loss factor of a similar building type postis used. As the prediction is affected as well by parameters such as the subsoil conditions and the measurement point, however, an accurate experimental prediction is not possible in every situation. The accuracy of the prediction could be improved by providing predictions of the coupling loss factor by means of numerical simulation, as has been shown in this paper. The advantage of the numerical prediction of the coupling loss factor is the greater flexibility in dealing with different building and founation configurations and soil properties, while the advantage of using experimental data of the source and the transfer of vibration is that the local conditions are correctly accounted for. A hybrid experimental–numerical prediction combines both advantages.

8 Conclusions

The FRA procedure is an empirical procedure for the prediction of railway induced vibration in buildings. The source, the wave propagation and the receiver are characterized experimentally by a force density, a line transfer mobility and a coupling loss factor, respectively. The line transfer mobility is determined directly based on wave propagation tests. The force density and the coupling loss factor are determined indirectly, however, and they are influenced by several parameters such as the subsoil conditions. Previously, the influence of the soil conditions and other parameters on the force density and the resulting prediction accuracy has been investigated [7]. In this paper, the influence of the soil conditions and the location of measurement points on the coupling loss factor of a specific building type has been investigated by means of a numerical simulation of the FRA procedure.

The coupling loss factor characterizes the modification of the vibration velocity level due to the dynamic soil–structure interaction at the receiver side. This effect, however, is dependent on the conditions of the subsoil. Generally, a higher reduction is obtained at a higher frequency and for softer soils. The dependency of the coupling loss factor on the soil conditions leads to an overestimation of the response in case of a coupling loss factor determined on a stiffer soil and an underestimation in case of a coupling loss factor determined on a softer soil. Furthermore, a large spatial variation is observed in the coupling loss factors determined at different points in the foundation of a building due to the kinematics of the building and local variations of the geometry.

As the coupling loss factor is influenced by several parameters such as the soil conditions and the location of the measurement point, it is important that experimental data of the coupling

loss factor is used on sites with similar conditions. An appropriate experimental coupling loss factor may not be available, making an accurate empirical prediction impossible. It has been shown in this paper that the coupling loss factor can also be predicted by means of numerical simulations and combined with an experimental prediction of the free field vibration velocity level. A hybrid experimental–numerical prediction method is then obtained that combines the advantages of both methods.

Acknowledgements

The first author is a Research Assistant of the Research Foundation - Flanders (FWO). Their financial support is gratefully acknowledged.

REFERENCES

[1] G. Lombaert, G. Degrande, J. Kogut, and S. François, "The experimental validation of a numerical model for the prediction of railway induced vibrations," *Journal of Sound and Vibration*, vol. 297, no. 3-5, pp. 512–535, 2006.

[2] X. Sheng, C.J.C. Jones, and M. Petyt, "Ground vibration generated by a load moving along a railway track," *Journal of Sound and Vibration*, vol. 228, no. 1, pp. 129–156, 1999.

[3] C.E. Hanson, D.A. Towers, and L.D. Meister, "High-speed ground transportation noise and vibration impact assessment," HMMH Report 293630-4, U.S. Department of Transportation, Federal Railroad Administration, Office of Railroad Development, October 2005.

[4] C.E. Hanson, D.A. Towers, and L.D. Meister, "Transit noise and vibration impact assessment," Report FTA-VA-90-1003-06, U.S. Department of Transportation, Federal Transit Admininistration, Office of Planning and Environment, May 2006.

[5] E.C. Bovey, "Development of an impact method to determine the vibration transfer characteristics of railway installations," *Journal of Sound and Vibration*, vol. 87, no. 2, pp. 357–370, 1983.

[6] J.T. Nelson and H.J. Saurenman, "A prediction procedure for rail transportation groundborne noise and vibration," *Transportation Research Record*, vol. 1143, pp. 26–35, 1987.

[7] H. Verbraken, H. Eysermans, E. Dechief, S. François, G. Lombaert, and G. Degrande, "Verification of an empirical prediction method for railway induced vibration," in *Proceedings of the 10th International Workshop on Railway Noise IWRN10*, Nagahama, Japan, October 2010, pp. 229–236.

[8] G. Lombaert and G. Degrande, "Ground-borne vibration due to static and dynamic axle loads of InterCity and high speed trains," *Journal of Sound and Vibration*, vol. 319, no. 3-5, pp. 1036–1066, 2009.

[9] S. François, M. Schevenels, G. Lombaert, P. Galvín, and G. Degrande, "A 2.5D coupled FE-BE methodology for the dynamic interaction between longitudinally invariant structures and a layered halfspace," *Computer Methods in Applied Mechanics and Engineering*, vol. 199, no. 23-24, pp. 1536–1548, 2010.

[10] K. Knothe and S.L. Grassie, "Modelling of railway track and vehicle/track interaction at high frequencies," *Vehicle Systems Dynamics*, vol. 22, pp. 209–262, 1993.

[11] S. François, *Nonlinear modelling of the response of structures due to ground vibrations*, Ph.D. thesis, Department of Civil Engineering, K.U.Leuven, 2008.

[12] Deutsches Institut für Normung, *DIN 45672 Teil 2: Schwingungsmessungen in der Umgebung von Schienenverkehrswegen: Auswerteverfahren*, 1995.